CONF-9501130--1

EXPERIMENTAL STUDY OF STATIC FLOW INSTABILITY IN SUBCOOLED FLOW BOILING IN PARALLEL CHANNELS*

M. Siman-Tov
D. K. Felde
J. L. McDuffee
G. L. Yoder
Oak Ridge National Laboratory
P.O. Box 2009
Oak Ridge, Tennessee 37831-8218

To be presented at the
4th ASME/JSME Thermal Engineers
Joint Conference
Maui, Hawaii
January 1995

---

*Research sponsored by the Office of Energy Research, U.S. Department of Energy, under contract DE-AC05-84OR21400 with Martin Marietta Energy Systems, Inc.

EXPERIMENTAL STUDY OF STATIC FLOW INSTABILITY IN SUBCOOLED FLOW BOILING IN PARALLEL CHANNELS

Moshe Siman-Tov
Dave K. Felde
Joel L. McDuffee
Graydon L. Yoder, Jr.

Engineering Technology Division
Oak Ridge National Laboratory[1]
Oak Ridge, Tennessee

ABSTRACT

Experimental data for static flow instability or flow excursion (FE) at conditions applicable to the Advanced Neutron Source Reactor are very limited. A series of FE tests with light water flowing vertically upward was completed covering a local exit heat flux range of 0.7–18 MW/m^2, exit velocity range of 2.8–28.4 m/s, exit pressure range of 0.17–1.7 MPa, and inlet temperature range of 40–50°C. Most of the tests were performed in a "stiff" (constant flow) system where the instability threshold was detected through the minimum of the pressure-drop curve. A few tests were also conducted using as "soft" (constant pressure drop) a system as possible to secure a true FE phenomenon (actual secondary burnout). True critical heat flux experiments under similar conditions were also conducted using a stiff system. The FE data reported in this study considerably extend the velocity range of data presently available worldwide, most of which were obtained at velocities below 10 m/s. The Saha and Zuber correlation had the best fit with the data out of the three correlations compared. However, a modification was necessary to take into account the demonstrated dependence of the St and Nu numbers on subcooling levels, especially in the low subcooling regime. Comparison of Thermal Hydraulic Test Loop (THTL) data, as well as extensive data from other investigators, led to a proposed modification to the Saha and Zuber correlation for onset of significant void, applied to FE prediction. The mean and standard deviation of the THTL data were 0.95 and 15%, respectively, when comparing the THTL data with the original Saha and Zuber correlation, and 0.93 and 10% when comparing them with the modification. Comparison with the worldwide database showed a mean and standard deviation of 1.37 and 53%, respectively, for the original Saha and Zuber correlation and 1.0 and 27% for the modification.

INTRODUCTION

The Advanced Neutron Source (ANS) is a state-of-the-art research facility that will be built at the Oak Ridge National Laboratory (ORNL). It is designed to become the world's most advanced facility for scientific experiments. To meet the scientific requirements, the core of the ANS reactor (ANSR), the neutron source, must be designed to accommodate very high power densities using a very large coolant mass flux and a high level of subcooling. A statistical/probabilistic uncertainty analysis is being performed to determine the optimal design power and to provide the necessary safety margin. This analysis requires selecting the most appropriate thermal-hydraulic (T/H) correlations and developing uncertainty distribution profiles based on the best available data as discussed by Siman-Tov et al. (1991).

In the baseline design, the ANSR is cooled and moderated by heavy water and uses highly enriched uranium silicide fuel. The core is composed of two coaxial annular core halves, of different diameters, each shifted axially with respect to the other. There are 684 parallel aluminum-clad fuel plates arranged in an involute geometry that effectively creates an array of thin rectangular flow channels with each plate being 1.27 mm thick. The coolant channels have 1.27 mm gap width, spans of 87 and 70 mm (lower and upper core, respectively), and a 507-mm heated length. Each fuel plate has a 10-mm unheated length at the leading and trailing edges, while all the channels connect to common inlet and outlet plenums with

nominal pressures of 3.2 and 1.7 MPa, respectively. The coolant flows vertically upward at an inlet velocity of 25 m/s, corresponding to a Reynolds number of 99,000, with average inlet and outlet temperatures of 45 and 85°C, respectively. The nominal average heat flux is 5.7 MW/m^2 with radial (spanwise) and axial distributions which peak at a nominal local maximum heat flux of 11 MW/m^2.

The ANSR core configuration with multi-parallel channels is subject to a potential static instability called flow excursion (FE), which differs from a true critical heat flux (CHF) that would occur at a fixed channel flow rate as discussed later. The available correlations and experimental databases for FE and CHF seldom include the specific combination of ANSR operating parameters (see Data Comparison and Correlation). In addition, many investigators in the past did not distinguish between FE and true CHF, adding to the inconsistencies in the available FE and CHF databases, since both are very complex but distinctly different phenomena (see discussion below).

The Thermal Hydraulic Test Loop (THTL) facility was designed and built to provide known T/H conditions in a full-length coolant subchannel of the ANSR core, thus facilitating experimental determination of FE and CHF thermal limits under expected ANSR T/H conditions. Determination of these two thermal limits and the relationship between them is the main objective of the THTL facility. This paper will discuss the initial experiments that focused on the FE phenomena, two CHF experiments performed for comparison, data evaluation and correlation, results, and recommendations.

EXCURSIVE FLOW INSTABILITY AND TRUE CRITICAL HEAT FLUX

The cooling channels in the ANSR fuel assembly are all parallel and share common inlet and outlet plenums, effectively imposing a common pressure drop across all the channels. This core configuration is subject to FE and/or flow instability (Leddineg 1938, 1949) that may occur once boiling is initiated in any one of the channels. The FE phenomenon constitutes a different thermal limit from a true CHF or departure from nucleate boiling (DNB). CHF is the state where the wall loses its direct contact with the liquid because of vapor accumulation, causing a temperature excursion that can lead to channel failure. In a system subject to FE, initiation of boiling in one of the channels (i.e., a hot channel) can result in flow redistribution to the other, cooler channels. This process can very rapidly lead to flow starvation in the hot channel, leading in turn to a local CHF or DNB at a flow lower than the core nominal flow rate. Along the channel there are three distinct zones. The first consists of convective single-phase flow where the pressure gradient actually decreases along the flow because of a reduction in fluid viscosity with increased temperature. In the second zone, which begins at the point of incipient boiling (IB), the pressure gradient rises very gradually until the onset of net vapor generation (ONVG) point or the point of onset of significant void (OSV), where both void generation and pressure gradient start increasing sharply. It is normally assumed that at the OSV point, bubbles begin to detach from the wall and move into the core of the fluid. In the third zone, both void generation and pressure gradient increase rapidly, leading to a rapid reduction of the coolant flow rate in the channel. The flow reduction promotes more boiling, which rapidly leads to FE [also referred to as the onset of flow instability (OFI)]. Because of the sharp acceleration in void generation occurring after OSV, the third zone is normally short. As a result, it is normally accepted that FE or OFI will most likely occur soon after OSV is established, which can thus serve as an early (conservative) warning to the expected occurrence of FE.

Maulbetsch and Griffith (1965) and other investigators have analytically and experimentally demonstrated the conditions under which excursive instability will occur. They determined that such instability will occur "if the slope of the (demand) pressure-drop vs. flow rate is more negative than that of the external supply system" which can be expressed mathematically as:

$$\frac{d(\Delta P_{ext})}{dQ} > \frac{d(\Delta P_{dem})}{dQ} \quad . \qquad (1)$$

Figure 1 presents a typical plot of the demand pressure-drop vs. flow rate relationship with various externally supplied boundary conditions. In the case of many parallel channels between large common headers, as is the case in the ANSR, the slope of the external supply system is practically zero (constant pressure drop) and OFI or FE conditions are determined by the minimum in pressure-drop, point (4), on the demand curve. Based on this observation, FE or OFI conditions were determined in most of the THTL FE experiments by detection of the test section pressure-drop minimum as the flow through the test section was reduced in steps under a constant heat flux. This method allowed for repetition of many non-destructive FE tests without experiencing an actual FE that normally causes test section failure. To be able to perform the tests in this mode, a "stiff" system was used where the bypass around the test section was closed or minimized to maintain a near-constant flow through the test section. In addition, a near positive-displacement pump that provides a nearly constant flow rate (a slope of about 10^{-4} m^3/s per MPa) was used in the primary loop. Small diameter piping (to reduce volume) and a throttling valve were also placed upstream from the test section inlet to enhance flow stability. For confirmation and comparison, limited experiments were performed with an actual FE burnout using a "soft" system. In this mode, a large bypass around the test section is fully open to maintain an almost constant common pressure-drop across the test section, thus closely simulating the ANSR configuration. Some experiments for true CHF burnout were also run in a stiff system (with the bypass completely closed) by reducing the flow until actual burnout occurred.

In most cases, FE will precede true CHF in a parallel channel configuration such as the ANSR (Waters 1966). It is noteworthy, however, that the margin between FE and CHF narrows as the level of certain parameters increases, and, at a certain point, the trend may even be reversed (Boyd 1988). Since the ANSR normally will operate at moderate pressures

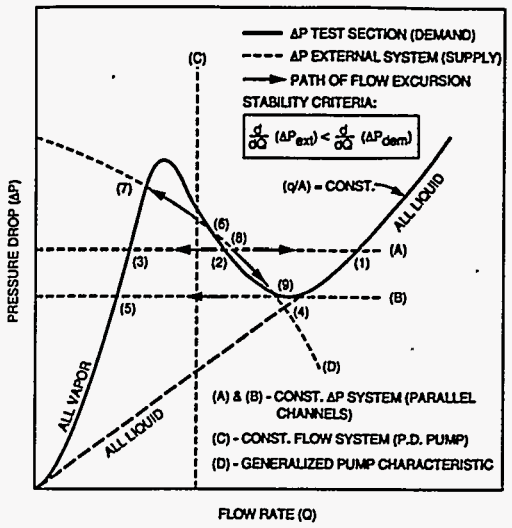

FIG. 1. SCHEMATIC INTERPRETATION OF EXCURSIVE INSTABILITY (MODIFIED FROM MAULBETSCH AND GRIFFITH 1965).

and very high mass flux and subcooling levels, one of the main goals of these tests is to determine the relationship between CHF and FE under ANSR conditions.

EXPERIMENTAL DESIGN AND PROCEDURES

The THTL was designed and built to provide known T/H conditions to a simulated full-length coolant subchannel of the ANSR core, allowing experimental determination of the FE and CHF thermal limits under anticipated ANS T/H conditions.(Felde et al. 1994). The test section simulates a single subchannel in the ANSR core with a cross section (Fig. 2) that has full prototypic length (507 mm), the same flow-channel gap (1.27 mm), and the same material (Al-6061) with a surface roughness (~0.5 μm) reasonably close to that expected in the ANSR fuel plates. The channel span was scaled down to 12.7 mm (vs. 87 and 70 mm for the upper and lower elements in the ANSR core) to limit the total power requirements to the test section. To simplify the experimental design and operation, the involute shape of the plates was not simulated. Other researchers have demonstrated that there is little spanwise fluid mixing in such rectangular channels even under two-phase flow conditions (Costa et al. 1967; Waters 1966). Furthermore, sources maintain that span width (or span to gap ratio) does not have a significant effect on either CHF or FE (Whittle and Forgan 1967; Gambill and Bundy 1964). The test section wall thickness was 2.54 mm, as dictated by the voltage/current characteristics of the available power supplies (later experiments will address axial and spanwise heat flux distributions). The reduced wall thickness at the curved ends

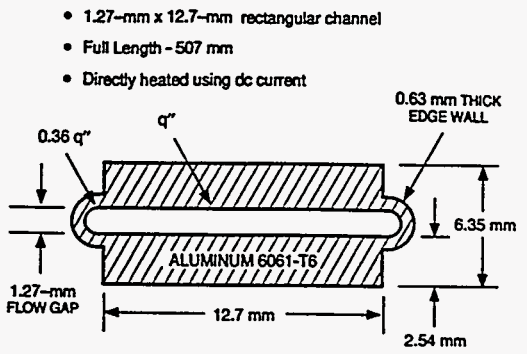

FIG. 2. CROSS-SECTION OF THE TEST CHANNEL IN THE THERMAL HYDRAULIC TEST LOOP.

was designed to lower the heat flux and prevent premature burnout in this area of the channel. The ratio of the heat flux on the curved ends to that on the flat section is 36%. The test channel thermocouples were placed on the back of the channel wall and measurements were made on both sides of the channel for redundancy.

FE tests (without burnout) were conducted in a stiff mode as described earlier. These tests were initiated by controlling test-section flow to a level where no boiling existed at the target heat flux level. The applied power to the test section was then raised to produce the target heat flux level. Exit pressure was automatically controlled via the system letdown valve and high-pressure make-up pump at the desired setting (nominally 1.7 MPa). Process water flow to the secondary side of the heat exchanger was also automatically controlled to maintain the inlet bulk coolant temperature at the desired setpoint (nominally 45°C). Once the system stabilized and data were obtained under steady-state conditions, the velocity was reduced in steps to lower levels while the differential pressure was monitored across the test channel. The minimum in pressure drop was determined by observation of the increasing pressure drop as velocity was decreased further; then, the velocity was increased again and data were taken for comparison at some of the velocity points obtained during the earlier sequence.

An experimental data reduction model was developed for single-phase forced-convection flow, focusing on the flat portion of the test channel. The test section surface temperature ($T_{w,in}$) on the flow channel side was determined based on the local internal heat generation in the channel flats and the corresponding measured external wall temperature ($T_{w,ex}$). The local internal heat generations and heat fluxes were calculated by the code based on voltage drop, current, and local resistivity. Heat losses, primarily through the flanges and electric busses on both sides of the test section, and internal heat redistribution in the axial and spanwise directions within the aluminum test section had to be estimated in order to deduce the actual local heat flux at the mid-plane where the thermocouples are placed. In addition, uncertainty in local

oxide layer buildup thickness required approximations, which affected some calculated local temperatures. Fortunately, the effect of those uncertainties on conditions important to FE prediction, such as velocity and bulk subcooling, was not large. Uncertainties were estimated by the root-sum-square method, including most of the measured and data reduction components with the results (at two standard deviations level) for the major parameters being L = ±4%, P = ±5.8%, T_b = ±2.0%, ΔT_{sub} = ±3.0%, Q = ±3.4%, G = ±5.4%, q''_{ex} = ±6.4%, and St = ±12.4%.

RESULTS AND DISCUSSION

The current THTL experimentation for the ANSR T/H correlations emphasizes the FE phenomenon and, to a lesser extent, CHF. The first goal was to proceed from low levels of heat flux and velocity and then extend the tests to the extremely high levels corresponding to the ANSR operating conditions. The initial phase of this activity was reported by Siman-Tov, et al. (1993). Since then, additional experiments have been performed that covered higher heat fluxes and velocities. The experiments completed so far include the following nominal T/H conditions:

- light water coolant,
- rectangular channel: 1.27 × 12.7 × 507 mm (Fig. 2),
- inlet coolant temperature: 45 (and 40)°C,
- exit coolant pressure: 1.7 (and 0.45, 0.17) MPa,
- exit heat flux range: 0.7–18 MW/m^2, and
- corresponding exit velocity range: 2.8–28.4 m/s.

A summary of the pertinent data from all the tests that led to minimum point (FE) conditions or actual burnout is given in Table 1. Plots of pressure-drop vs. mass flux for each of those tests are shown in Fig. 3. The heat fluxes indicated for each test in Fig. 3 correspond to the channel average values at the minimum pressure drop point of that specific test (corresponding values are shown in Table 1 as q''_{avg}). The actual local heat fluxes close to the exit where the FE phenomena is supposed to occur are indicated in Table 1 as q″ These heat flux values at the exit are higher than the average as a result of the temperature dependence of the aluminum electrical resistivity. As illustrated in Fig. 3, the minimum points could be clearly detected, and it can also be seen that the limiting velocities of those points are obviously increasing for higher heat fluxes. In none of these tests was a true CHF (or the subsequent expected burnout) encountered before the minimum point was reached where FE is supposed to occur.

In addition to the above non-destructive FE experiments, a number of destructive (actual burnout) tests were performed using a soft system to determine the effect of bypass ratio on FE conditions. Three such destructive FE tests were performed and the results are presented in Fig. 4. The FE318B test was designed to provide benchmark FE data under conditions similar to those used in attaining the Costa (1967) data. As can be seen in the figure, the minimum pressure-drop point was achieved at a velocity of 4.7 m/s compared with 5.4 m/s in Costa, which is a reasonable agreement.

Tests FE212A and FE331A allowed investigation of the effect of bypass ratio on the actual FE burnout in relation to the minimum point in each. Both tests are for a nominal average heat flux of 12 MW/m^2, but FE212A had a bypass ratio of 2.6 while FE331A used 6.2, the highest bypass possible for the loop at that velocity. The minimum pressure drop points were achieved at 19.3 and 19.5 m/s, respectively, showing the anticipated close agreement. However the actual destructive FE failures came at velocities of 17.8 m/s for the FE212A test (bypass ratio of 2.6) and 18.4 m/s for the FE331A test (bypass ratio of 6.2), both at lower velocities than the corresponding minimum points. This comparison is consistent with expectations that higher bypass ratios should cause the actual FE to approach closer to the minimum point. The minimum pressure drop technique for determining FE conditions is clearly a conservative estimate since it implies an ideally constant pressure drop boundary condition, as would be the case for an "infinite bypass."

Two CHF experiments, CF115B and CF328A, were performed in a stiff system with a closed bypass line by further reducing the velocity after the minimum pressure-drop point was achieved. Both experiments were conducted under similar conditions with average heat fluxes of 10.5 and 11.8 MW/m^2, respectively. The results are presented in Fig. 4 with the rest of the burnout cases. The occurrence of CHF was clearly identified in the experiments by a rapid burnout and failure of the test channel. The CHF showed a 30% additional margin in velocity (14.5 m/s) compared with the FE velocity of 19.8 m/s corresponding to the minimum pressure-drop point. This margin between FE and CHF was surprisingly large based on the values predicted by the respective correlations. As expected, a destructive FE did not occur before the CHF point, confirming that flow instability does not occur in a stiff system (constant flow), as discussed earlier.

Acquiring FE data at these heat fluxes and velocities is significant for two reasons. First, to the authors' knowledge, very little data is available for FE at velocities higher than 10 m/s [the few exceptions are by Waters (1966), Maulbetsch and Griffith (1965), and Croft (1964)] and none at all are known above 18 m/s. The range of data has now been extended to a velocity of 28.4 m/s (at the exit), which is above the maximum velocity expected in the ANSR, including uncertainties. Second, the high heat flux achieved in this study (16.8 MW/m^2 average and 17.9 MW/m2 at the exit) is well above the ANSR nominal average heat flux of 5.9 MW/m^2 and nominal peak heat flux of 12 MW/m^2. In fact, it is almost as high as the ANSR local "hot channel peaking factor" heat flux (e.g., peak heat flux with uncertainties) of 18 MW/m^2. The limiting velocity corresponding to the ANSR nominal peak of 12 MW/m^2 is about 20 m/s (at a subcooling of 23°C), well below the ANSR nominal velocity of 25 m/s. The limiting heat flux corresponding to this nominal velocity is 15.5 MW/m^2 (at a subcooling of 20°C), considerably above the ANSR nominal peak heat flux. Furthermore, the two true CHF tests performed at the nominal heat flux provided an additional margin relative to the ANSR nominal velocity for the CHF thermal limit.

TABLE 1. THTL CRITICAL DATA POINTS FOR FLOW EXCURSION AND CHF TESTS

TSD	q''_{avg} Test Case	q'' (MW/m^2)	q'' (MW/m^2)	V (m/s)	ΔP_{ts} (MPa)	P (MPa)	T (°C)	ΔT_{sub} (°C)	Heat Loss %
TSD-3/C	FEN17B	7.6	7.9	14.4	0.296	1.721	182.5	22.7	7.6
TSD-3/C	FEN17C	10.6	11.3	20.0	0.508	1.693	178.1	26.4	6.4
TSD-3/C	FEN20A	12.0	13.6	21.9	0.604	1.725	178.6	26.9	6.3
TSD-3/C	FEN20B	13.7	16.0	23.5	0.742	1.712	180.0	25.2	4.8
TSD-3/C	FEN30A	13.6	15.8	23.6	0.754	1.709	180.7	24.4	4.6
TSD-3/C	FED15B	11.6	13.0	19.7	0.545	1.706	181.9	23.0	5.5
TSD-3/C	FED15C	13.0	14.7	21.4	0.632	1.719	181.3	24.1	5.1
TSD-3/C	FED17A	14.4	16.1	23.5	0.747	1.685	176.8	27.7	6.1
TSD-3/C	FED28B	14.6	15.5	23.0	0.765	1.723	181.1	24.4	5.5
TSD-3/C	FE105B	9.0	9.9	15.4	0.359	1.721	173.6	31.6	6.2
TSD-3/C	FE105C	12.7	14.3	20.1	0.657	1.722	179.1	26.3	4.9
TSD-3/C	FE105D	14.8	16.3	23.1	0.919	1.707	182.5	22.6	4.4
TSD-3/D	FE114B	10.8	11.8	20.1	0.567	1.713	181.9	23.2	4.8
TSD-3/D	CF115B	11.8	13.0	19.8	0.628	1.709	186.1	18.9	4.2
TSD-3/D	CF115B*	11.8	13.0	14.5	1.262	1.860	209.2	-0.5	4.5
TSD-3/E	FE210B	11.4	13.9	20.1	0.618	1.718	178.2	27.1	5.9
TSD-3/E	FE212A	12.1	13.3	19.3	0.653	1.708	185.2	19.7	5.6
TSD-3/E	FE212A*	12.1	13.0	17.8	0.785	1.738	194.8	10.6	7.4
TSD-3/F	FE318B	1.9	2.2	5.0	0.078	0.445	132.7	15.1	12.4
TSD-3/F	FE318B*	2.1	2.3	4.5	0.106	0.451	142.2	6.0	16.4
TSD-3/G	FE330A	12.0	14.0	21.1	0.577	1.709	174.7	30.3	3.6
TSD-3/G	FE331A	12.0	13.7	19.6	0.549	1.698	178.4	26.3	8.8
TSD-3/G	FE331A*	11.5	12.4	18.3	0.634	1.708	181.8	22.8	9.6
TSD-3/J	FE712B	1.7	1.9	2.9	0.033	1.695	183.1	21.1	12.2
TSD-3/J	FE713B	0.7	0.7	2.8	0.025	0.175	100.1	16.2	15.1
TSD-3/J	FE714B	4.3	5.0	8.6	0.142	1.700	174.3	30.2	6.5
TSD-3/J	FE714C	6.4	7.2	11.6	0.248	1.701	182.3	22.2	5.5
TSD-3/J	FE715B	9.2	10.8	16.6	0.440	1.709	177.0	27.9	3.1
TSD-3/J	FE719B	11.7	14.8	20.1	0.634	1.673	176.8	27.1	3.8
TSD-3/K	FE324C	5.6	6.5	9.4	0.137	1.726	182.8	22.0	7.7
TSD-3/K	CF328A	12.3	13.8	19.3	0.592	1.715	181.2	23.6	6.7
TSD-3/K	CF328A*	10.5	11.0	14.0	1.098	1.850	208.8	-0.3	6.2
TSD-3/L	FE511B	14.7	15.5	25.0	1.074	1.700	185.8	20.3	5.2
TSD-3/L	FE511C	16.8	17.9	28.4	1.432	1.680	184.3	21.6	5.2

1. In all cases the inlet temperature is nominally 45°C, except for FE318B where the inlet temperature is 40°C.
2. The critical point refers to the minimum pressure drop data point for most flow excursion tests. The asterisk (*) symbol refers to a true destructive burnout.

DATA COMPARISON AND CORRELATION

The collected THTL data were compared with correlations by Costa (1967), Whittle and Forgan (W&F) (1967), and Saha and Zuber (S&Z) (1974) as shown in Fig. 5. The Costa correlation is the one currently being used for the preliminary ANSR T/H design and analysis. The W&F and S&Z correlations are widely used in the United States; the S&Z correlation is well established in many computer codes for nuclear safety analysis. For a given coolant (water), physical properties, and geometry (L/D = 199.6), all three original correlations can be rearranged and simplified to the same general formulation as follows:

$$q''_{fe}/(T_s - T_b)_{fe} = CV^n \quad , \qquad (2)$$

where c = 1/0.0128 and n = 0.5 (Costa); c = 1/0.0382 and n = 1.0 (S&Z); c = 1/0.0427 and n = 1.0 (W&F).

In the Costa correlation, the FE heat flux is proportional to the square root of velocity, whereas both W&F and S&Z (as well as most other FE correlations) have a linear dependence. Based on this formulation, the Costa correlation will yield the

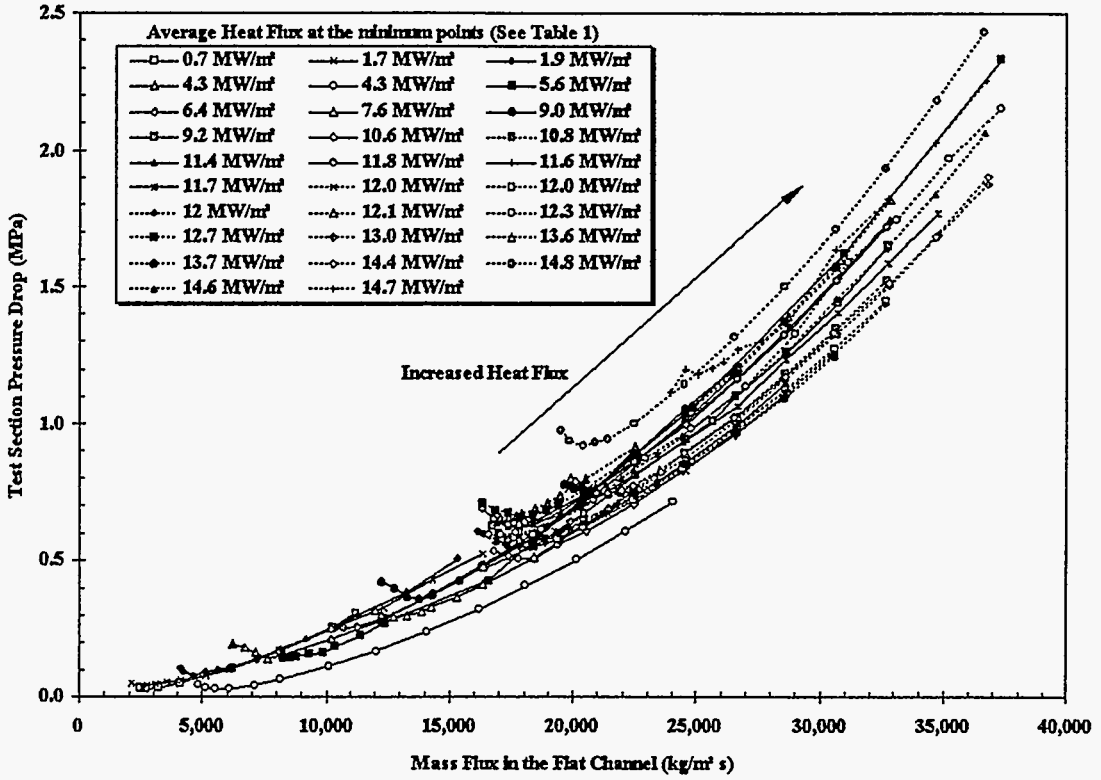

FIG. 3. FLOW EXCURSION DATA FROM THERMAL HYDRAULIC TEST LOOP EXPERIMENTS.

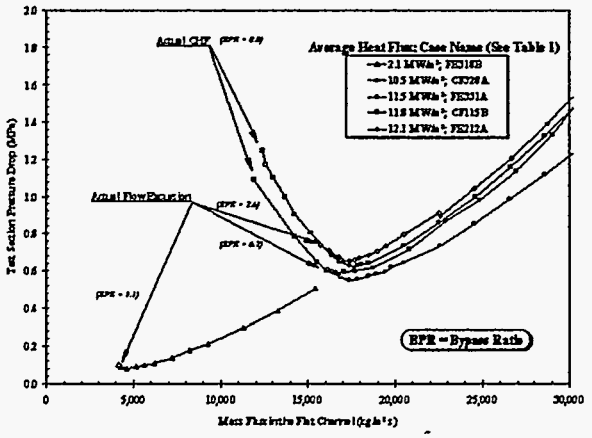

FIG. 4. DESTRUCTIVE CRITICAL HEAT FLUX AND FLOW EXCURSION TEST DATA FROM THE THERMAL HYDRAULIC TEST LOOP.

same result as the S&Z correlation at a velocity of 8.9 m/s and, in comparison, will be more optimistic (higher heat flux) at lower velocities and overly conservative at higher velocities (40% more conservative than S&Z at the ANSR nominal velocity of 25 m/s). The Costa correlation shows similar trends when compared with the W&F correlation. All three correlations seem to be generally conservative when compared with the data, with the S&Z correlation having the closest fit. The Costa correlation compares reasonably well with the THTL data in the low-velocity range (below 10 m/s) of the Costa (1967) data, but it becomes increasingly conservative as the velocity increases. The FE heat flux dependence on velocity seems to be between 0.5 power (Costa) and 1.0 (S&Z and W&F), more nearly in the 0.8–0.9 range. This trend is in agreement with the conclusions arrived at by Lee and Bankoff (1992) and Rogers & Li (1992) who relate the heat flux at FE to the turbulent heat-transfer coefficient, which is approximately proportional to the 0.6–0.8 power of velocity.

The above data comparison and discussion supports a shift from the Costa correlation to the S&Z correlation for the ANSR, especially since the nominal conditions of most of the accident scenarios analyzed in the ANSR involve quite high mass fluxes. The W&F correlation, although a reasonable selection based on direct data comparison, was not selected because of its global rather than local nature. This characteristic of the W&F correlation becomes a major liability for non-uniform heat flux distributions as exist both axially and spanwise in the ANSR, and when statistical uncertainties are applied in the analysis. tThe S&Z correlation seems to be a

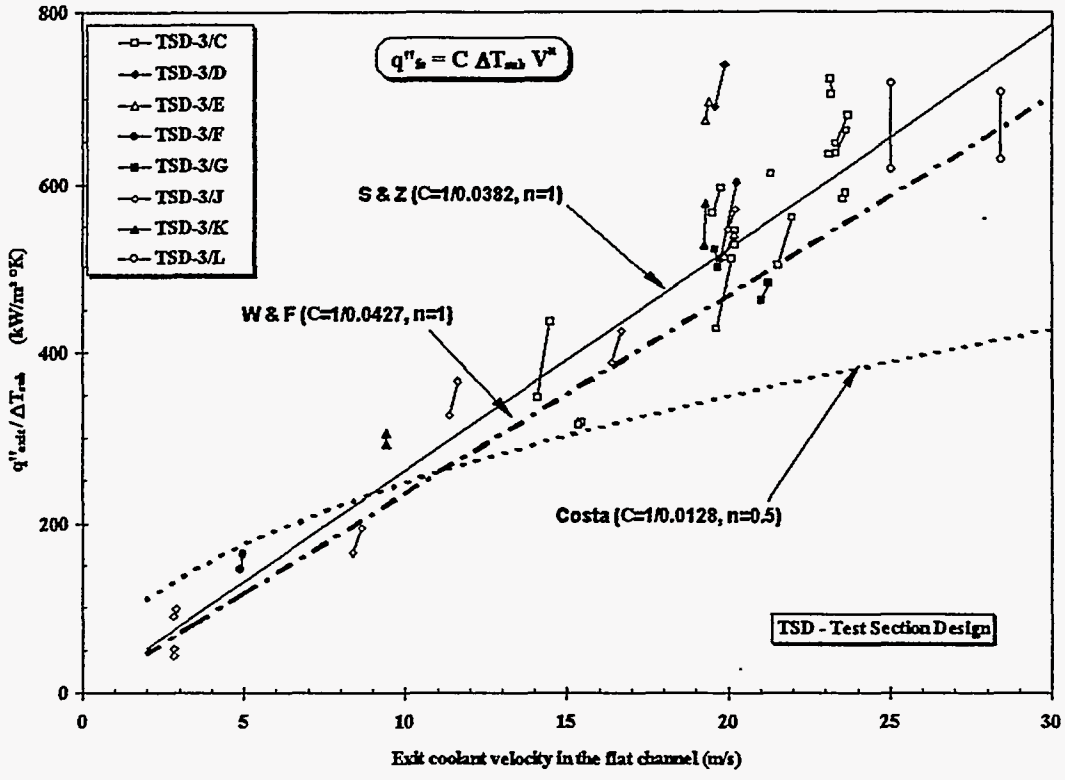

FIG. 5. COMPARISON OF FLOW EXCURSION DATA FROM THERMAL HYDRAULIC TEST LOOP EXPERIMENTS. BARS REPRESENT UNCERTAINTY RELATED TO AXIAL AND LATERAL INTERNAL HEAT REDISTRIBUTION BY CONDUCTION.

good selection for the ANSR conditions because it represents the data quite well over the entire range of interest. However, the limiting heat flux based on the original S&Z correlation is very sensitive tohe subcooling value at low subcooling and decreases rapidly to zero as subcooling gets to zero. This is obviously unrealistic since the flow excursion heat flux cannot be lower than the incipient boiling heat flux. Therefore, it became useful to plot both the THTL data and the rest of the ANS database for FE [see Table 2 and Siman-Tov, et al. (1991)] in terms of the St number that is the selected dimensionless group for Pe > 70,000 in the original S&Z correlation against subcooling as shown in Fig. 6. As can be seen in the figure, there is a clear trend for the St number to increase with declining subcooling, particularly at lower subcoolings. In addition, it should be observed that *by definition* both the St number and the Nu number must become infinite when the subcooling is zero, contradicting the constant values for these parameters as suggested by the original S&Z correlation. This observation, in combination with the trend observed in the data, provides a strong case for modifying the S&Z constant St number (0.0065) and constant Nu number (455) criteria, especially in the low subcooling range. A best fit with the ANS database (including the THTL data) was developed which was constrained by the following criteria:

(1) Keep the original format of the S&Z correlation, that is, the use of St and Nu numbers as the main dimensionless groups.
(2) Keep continuity in switching from St number to Nu number at Pe = 70,000.
(3) Lean toward the conservative whenever necessary.
(4) Have both the St number and the Nu number tend toward infinity as the subcooling approaches zero to stay consistent with their definitions, yet avoid the heat fluxes vanishing to zero at subcooling equal to zero.
(5) Keep the correlation as close as possible to the original St number (0.0065) for the high subcooling range (up to 120°C) even though there are no data available beyond 50°C subcooling for the St number or beyond 25°C for the Nu number.
(6) Keep the uncertainties to a minimum and as uniform as possible for a broad range of the main T/H parameters to avoid the need for different standard deviations for different regimes.
(7) Recognize that the data available for the Nu number (Pe < 70,000) are limited.

TABLE 2. SUMMARY OF FE/OSV DATABASE USED IN PRESENT ANALYSIS

Author (year), organization	Number of data points	Velocity (m/s)	Pressure (MPa)	ΔT_{sub} (°C)	Heat flux (MW/m^2)
THTL	26	2.8–23.6	0.18–1.74	15.1–31.6	0.7–14.8
Lafay et al. (1965)	34	0.5–4.5	0.17	2.1–25.0	0.3–2.4
Lafay and Costa et al. (1967)	117	2.2–7.7	0.17–0.39	2.3–42.1	0.7–4.6
Courtaud et al. (March 1966)	6	2.5–9.0	0.3	11.3–22.2	2.0–4.0
Courtaud et al. (Jan. 1966)	15	1.8–7.0	0.28–0.32	11.8–24.7	2.0–4.0
Courtaud et al. (June 1967)	12	4.8–8.8	0.29–1.08	11.0–22.4	4.0–7.0
Vernier (1965)	19	2.1–10	0.15–0.29	6.6–16.5	1.0–4.5
Courtaud et al. (June 1966)	12	2.0–6.2	0.3	17.6–47.2	2.0–4.0
Whittle and Forgan (1967)	23	1.6–4.5	0.10–0.12	3.7–9.7	0.7–2.1
Whittle and Forgan (1967)	65	0.8–11.4	0.12–0.17	4.6–16.3	0.4–3.5
Schleisiek and Dumaine (1966)	14	3.6–9.0	0.39–0.49	11.2–18.8	2.5–5.1
Lafay et al. (1968)	18	1.6–9.2	0.49	5.4–33.6	2.0–6.0
Waters (1966)	18	0.5–17.8	0.27–2.52	6.0–24.6	0.1–6.5
Cheh and Fighetti (1990)	86	1.3–7.9	0.24–0.46	2.2–43.7	1.1–3.2
Egan (1957)	7	0.5–1.3	0.41-1.65	4.4–21.1	0.4–1.6
Ferrel (1964)	11	0.1–1.4	0.98-5.0	10.6–18.9	0.2–0.7
Griffith et al. (1958) BETTIS	12	0.5–1.2	8.2-13.6	6.1–41.7	0.3–1.9
Rouhani (1965) BMI	11	0.5–1.1	13.8	11.1–32.2	0.3–0.9

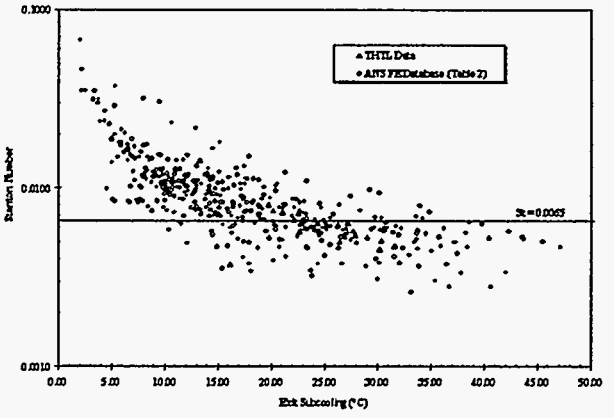

FIG. 6. DEPENDENCE OF CRITICAL St NUMBER ON SUBCOOLING LEVEL.

Under these criteria and constraints, the following subcooling correction factor seem to provide an improvement in the original S&Z correlations for the ANS applications:

$$St = q''/\left(GC_p\Delta T_{sub}\right) = 0.0065\eta_{sub}$$

$$= 0.0065\left[0.55+11.21/\left(\Delta T_{sub}\right)\right], \quad (Pe > 70{,}000) \quad (3)$$

$$Nu = q''D_h/\left(k\Delta T_{sub}\right) = 455\eta_{sub}$$

$$= 455\left[0.55+11.21/\left(\Delta T_{sub}\right)\right], \quad (Pe > 70{,}000) \quad (4)$$

where η_{sub} is the proposed subcooling correction factor. Figure 7 shows the selected modified correlations in terms of St number and Nu number, respectively, against the ANS database, including the THTL data of the present study. Table 3 provides the statistics for the modified S&Z correlation in terms of mean and standard deviation, as well as for the original S&Z and Costa correlations. The following comments should be noted concerning the proposed modification:

(1) As seen in Table 3, the modified S&Z correlation provides considerable improvement in the uncertainties compared with either the original S&Z correlation (especially at low subcooling) or the Costa correlation (especially at high velocities).

(2) The data currently available to us are limited to subcoolings less than 50°C for St and less than 25°C for Nu. The modified correlations were extrapolated beyond this data range to above 100°C to accommodate the range called for by various transient scenarios in the ANSR RELAP5 analysis.

(3) Even though the modified correlations are based on the original S&Z approach (using St and Nu as the criteria) for predicting the OSV point, they were modified based on a mixture of actual FE and OSV data. Therefore, the modified correlations here are probably more reflective of flow excursion than of OSV.

(4) It is worth indicating that the uncertainties shown in Table 3 are based on the database available at the present time (Table 2). With additional analytical work and in-house experimental efforts, these uncertainties could be reduced, especially those for Nu number.

(5) The large uncertainties currently shown for the Nu number are obviously impractical for application to very low safety margins, where two to three standard deviations are used. It is therefore necessary in those cases to eliminate unrealistic situations by conservatively using the incipient boiling criteria (or even the more conservative but simpler to use criterion of $T_w = T_{sat}$) as the lowest limit for all FE predictions.

SUMMARY AND CONCLUSIONS

1 A modification factor for the S&Z correlation FE was proposed to take into account the trend of increased values of St and Nu numbers with reduced subcooling and to be consistent with the *definition* of these two parameters. The proposed modification provides better

Gambill W. R., and Bundy, R. D. 1964. "Heat Transfer Studies of Water Flow in Thin Rectangular Channels, Part I: Heat Transfer, Burnout, and Friction for Water in Turbulent Forced Convection." *Nucl. Science and Eng.*, 18: 69–79.

Griffith, P., Clark, J. A., and Rohsenow, W. M. 1958. "Void Volumes in Sub-cooled Boiling." ASME Paper 58HT-19, U.S. National Heat Transfer Conference, Chicago, Ill.

Lafay, J., Maisonnier, G., and Girard, F. 1965. "Compte rendu d'essais flux de redistribution de debit—expulsion et calefaction—a basse pression et qux faibles bitesses en canal rectangulaire," TT/65-17-B/JL-GM-FG.

Lafay, J., Maisonnier, G., and Mazzili, F. 1968. "Compte rendu d'essais Influence de la repartition axiale du flux sur les seuils d'apparition de la redistribution de debit," TT/68-4-B/JL.

Leddineg, M. 1938. "Unstabitit der Stromung bei naturlic–en und Zwangumlauf." *die Warme,* 61(48): 891-898.

Leddineg, M. 1949. "Flow Distribution in Forced-Circulation Boilers," *The Engineering Digest,* 10: 85–89.

Lee, S. C. and Bankoff, S. G. August 1992. "Prediction of the Onset of Significant Void in Down Flow Subcooled Nucleate Boiling." In ASME HTD, Vol. 197, *Proc. of 28th National Heat Transfer Conference and Exhibition.* San Diego, Calif.

Maulbetsch, J. S. and Griffith, P. 1965. "A Study of System-Induced Instabilities in Forced-Convection Flows with Subcooled Boiling," Report No. 5382-35. Department of Mechanical Engineering Massachusetts Institute of Technology, Cambridge, Mass.

Rogers, J. T. and Li, J. 1992. "Prediction of the Onset of Significant Void in Flow Boiling of Water." In ASME HTD. Vol. 217, Winter Annual Meeting, Anaheim, Calif.

Rouhani, S. Z. 1965. "Void Measurement in the Region of Subcooled and Low Quality Boiling." Symposium on Two-Phase Flow, University of Exeter.

Saha, P. and Zuber, N. 1974. "Point of Net Vapor Generation and Vapor Void Fraction in Subcooled Boiling." In *Proc. of 5th Int. Heat Transfer Conf.*, 175–179. IV. Tokyo.

Schleisiek, K., and Dumaine, J. C. 1966. "Compte rendu d'essais Essais preliminaires pour RHF Determination experimentale des conditions de redistribution de debit aux pressions entre 4 et 5 kg/cm^2 abs pur un canal rectangulaire de 2 mm d'epaisseur et de 60 cm de longueur," TT/66-10-B/KS/JCD, 27.

Siman-Tov, M., et al. December 1991. "Thermal-Hydraulic Correlations for the Advanced Neutron Source Reactor Fuel Element Design and Analysis." In ASME HTD, Vol. 190, Winter Annual Meeting, Atlanta.

Siman-Tov, M., et al. 1993. "Experimental Investigation of Thermal Limits in Parallel-Plate Configuration for the ANSR," *29th National Heat Transfer Conference*, AIChE Vol. 89, 86–97, Atlanta.

Vernier, P. 1965. "Compte rendu d'essais Osiris—etude de surete determination experimentale de courbes en s et des conditions de redistribution de debit," TT/65-19-B/PV.

Waters, E. D. 1966. "Heat Transfer Experiments for Advanced Test Reactor," BNWL-216, UC-80 (TID-4500).

Whittle, R. H. and Forgan, R. 1967. "A Correlation for the Minima in the Pressure Drop vs. Flow-Rate Curves for Sub-Cooled Water Flowing in Narrow Heated Channels." *Nuclear Eng. & Design,* 6: 89–99.

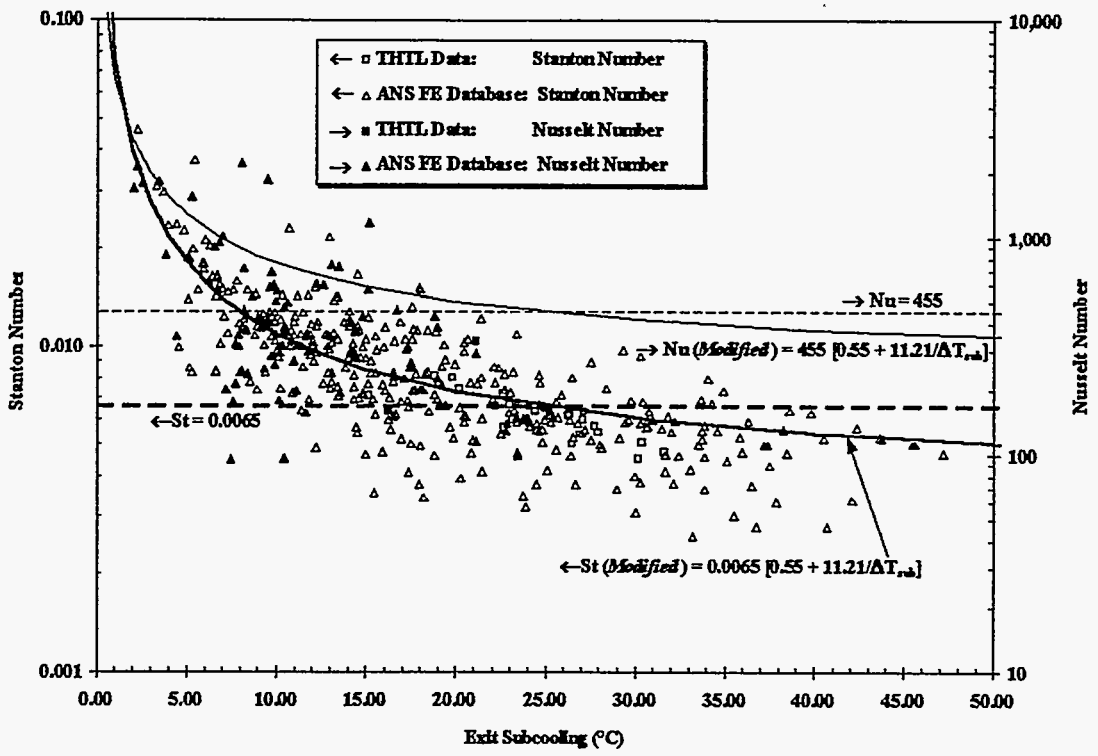

FIG. 7. COMPARISON BETWEEN THE MODIFIED AND UNMODIFIED FORMS OF THE SAHA ZUBER CORRELATION.

agreement and smaller standard deviations than either the Costa or the original S&Z correlation, based on both the THTL data and the broader ANS database.

2 Acquiring FE data at this level of heat flux and velocity is of great significance for numerous reasons. Most of the available FE data are in the low velocity range (<10 m/s) and none are available above 18 m/s. The data reported in this paper extend this data range up to 28.4 m/s (well beyond the ANSR nominal velocity of 25 m/s). The heat flux achieved in this study (16.8 MW/m^2 average and 17.9 MW/m^2 at the exit) is also well above the ANSR nominal average and peak heat fluxes of 5.9 and 12 MW/m^2, respectively, and almost as high as the ANSR "hot channel peaking factor" heat flux (peak heat flux with uncertainties) of 18 MW/m^2.

3. A true CHF (or the subsequent expected burnout) was not encountered before the minimum pressure drop (FE) point in any of the experiments performed thus far. Furthermore, the two true CHF tests performed at a nominal 12 MW/m^2 showed a 5 m/s (close to 30%) further reduction in limiting velocity compared with the corresponding FE tests, providing an additional margin relative to the ANSR nominal velocity for the CHF thermal limit.

4. Although a modification to the S&Z correlation was proposed for FE prediction, final correlation of the data for FE and CHF as a function of the major T/H parameters at the ANSR conditions range will be postponed until additional experiments and data analyses are performed.

ACKNOWLEDGMENT

The authors would like to acknowledge the support of the ANS Project Office that made this work possible and the help received from George Farquharson, Lara James, Marshall McFee, Bill Nelson, Professor Art Ruggles, and other contributors.

NOTATION

C = a constant [Eq. 2]
C_p = mean coolant specific heat (kJ/kgK)
D_h = heated diameter (m)
G = mass flux (kg/m^{2}s)
k = thermal conductivity (kW/mK)
Nu = nusselt number = $\frac{q''D_h}{k\Delta T_{sub}}$
P = pressure (Pa)

TABLE 3. U FACTOR[a] STATISTICS FOR COSTA, SAHA AND ZUBER, AND MODIFIED SAHA AND ZUBERCORRELATIONS

Peclet range	Correlation	Data range	Number points	Average	S.D.[b]	S.D.%
Pe > 70,000 (Stanton Correlation)	Costa	*THTL data*	24	1.452	0.326	22.45%
		All data	403	1.042	0.596	57.20%
		V > 8 m/s	46	1.679	0.609	36.25%
		V < 8 m/s	357	0.960	0.543	56.60%
	Saha and Zuber	*THTL data*	24	0.951	0.142	14.98%
		All data	403	1.375	0.722	52.51%
		V > 8 m/s	46	1.276	0.531	41.64%
		V < 8 m/s	357	1.388	0.743	53.52%
	Modified Saha and Zuber	*THTL data*	24	0.933	0.093	9.92%
		All data	403	1.000	0.274	27.43%
		V > 8 m/s	46	0.991	0.163	16.41%
		V < 8 m/s	357	1.001	0.286	28.56%
Pe < 70,000 (Nusselt Correlation)	Saha and Zuber	*THTL data*	2	0.535	0.267	49.96%
		All data	56	1.328	1.185	89.23%
	Modified Saha and Zuber	*THTL data*	2	0.474	0.277	58.30%
		All data	56	0.679	0.481	70.92%

[a]U = Experimental heat flux/predicted heat flux.
[b]S.D. = Standard deviation.

Pe = Peclet number = $\frac{Nu}{St} = \frac{GC_pK}{D_h}$

Q = flow rate (m^3/s)

q″ = heat flux (kW/m^2)

St = Stanton number = $\frac{q''}{GC_p\Delta T_{sub}}$

T = temperature (K)

ΔT_{sub} = subcooled temperature difference = $T_s - T_b$ (K)

V = coolant velocity (m/s)

n = exponential constant [Eq. 2]

ΔP = pressure drop (Pa)

η_{sub} = subcooling correction factor for the S&Z correlation (Eqs. 3 and 4)

Subscripts

avg = average across and along the test section
b = bulk coolant
dem = demand side
fe = at the flow excursion point
ex = exit
ext = external
in = inside
s = saturated
sub = subcooling
ts = test section
w = wall

LITERATURE CITED

Boyd, R.D. January 1985. "Subcooled Flow Boiling Critical Heat Flux (CHF) and Its Application to Fusion Energy Components. Part I: Fundamentals of CHF," and Part II: A Review of Microconvective, Experimental, and Correlational Aspects." *Fusion Tech.*, (7) 1.

Boyd, R.D. January 1988. "Subcooled Water Flow Boiling Experiments Under Uniform High Flux Conditions." *Fusion Tech.*, 13: 131–142.

Cheh, H. Y., and Fighetti, C. F. 1990. "Flow Excursion Experimental Program Single Tube Uniformly Heated Tests," CU-HTRF-T4.

Costa, J. 1967. "Measurement of the Momentum Pressure Drop and Study of the Appearance of Vapor and Change in the Void Fraction in Subcooled Boiling at Low Pressure," ORNL/TR-90/21. Martin Marietta Energy Systems, Inc., Oak Ridge National Laboratory. Oak Ridge, Tenn.

Costa, J., Courtaud, M., Elberg, and Lafay. 1967. "Flow Redistribution in Research Reactors," ORNL/TR-90/13. Martin Marietta Energy Systems, Inc., Oak Ridge National Laboratory. Oak Ridge, Tenn.

Croft, M. W. 1964. "Advanced Test Reactor Burnout Heat Transfer Test," ATR-FE-102 Babcock & Wilcox.

Courtaud, M., Coulon, G., and Mazzili, F. January 1966. "Compte rendu d'essais, boucle casimir Trace de courbes en S lere partie Eau degazee," TT/66-2-B/MC-GC/FM.

Courtaud, M., Coulon, G., and Mazzili. March 1966. "Compte rendu d'essais, boucle casimir Trace de courbes en S (Canal de 900 MM) Essais de depressurization," TT/66-7-B/MC-GC-FM.

Courtaud, M., Coulon, G., and Mazzili, F. June 1966. "Compte rendu d'essais, boucle casimir Trace de courbes en S sur des canaux a flux non uniforme," TT/66-14-B/MC-GC-FM.

Courtaud, M., Schleisiek, K., Coulon, G., and Mazzili, F. June 1967. "Compte rendu d'essais Pertes de charge de redistribution de debit sur des canaux rectangulaires de 1.8 mm d'entrefer (Type R.H.F.)," TT/67-7-B/MC-IS-GC-FM.

Egen, R. A., Dinger, D. A., and Chastain, J. W. 1957. "Vapor Formation and Behavior in Boiling Heat Transfer," BMI 1163.

Felde, D. K. et al. 1994. "Advanced Neutron Source Reactor Thermal-Hydraulic Test Loop Facility Description," ORNL/TM-12397. Martin Marietta Energy Systems, Inc., Oak Ridge National Laboratory, Oak Ridge, Tenn.

Ferrel, J. K. 1964. "A Study of Convection Boiling Inside Channels." Ph.D. Thesis, Department of Chemical Engineering, North Carolina State University, Raleigh, N.C.

DISCLAIMER